Polyhedron 29 (2010) 3342–3348

Contents lists available at ScienceDirect

Polyhedron

journal homepage: www.elsevier.com/locate/poly

Cluster based copper(II)-azide polymer: Synthesis, structure and magnetic study

Sandip Saha [a,*], Debabrata Biswas [a], Partha Pratim Chakrabarty [a], Atish Dipankar Jana [b], Athanassios K. Boudalis [c], Saikat Kumar Seth [d,e], Tanusree Kar [d]

[a] Department of Chemistry, Acharya Prafulla Chandra College, New Barrackpur, Kolkata 700 131, India
[b] Department of Physics, Behala College, Parnashree, Kolkata 700 060, India
[c] Institute of Materials Science, NCSR "Demokritos", 153 10, Aghia Paraskevi Attikis, Greece
[d] Department of Materials Science, Indian Association for the Cultivation of Science, Jadavpur, Kolkata 700 032, India
[e] Department of Physics, M.G. Mahavidyalaya, Bhupatinagar, Midnapore(E), West Bengal 721425, India

ARTICLE INFO

Article history:
Received 15 August 2010
Accepted 9 September 2010
Available online 22 September 2010

Keywords:
Ethylene diamine
Azides
Copper(II)
1D coordination polymers
Crystal structure
Magnetic properties

ABSTRACT

The reaction of ethylene diamine with $Cu(NO_3)_2\cdot 3H_2O$ and an excess of NaN_3 (1:2:4 molar ratio) lead to the formation of copper-azido based polymer $[Cu_4(N_3)_8(en)_2]_n$ (**1**), which has been successfully characterized by elemental analyses, IR spectroscopy, single-crystal X-ray diffraction and variable temperature magnetic study. X-ray crystal structure determination of **1** reveals that the structure consists of 1D chains of a centrosymmetric tetranuclear copper(II)-azido cluster, connected through double azido end-to-end bridges. Variable-temperature magnetic studies (between 2 and 300 K) suggest dominant antiferromagnetic interactions in this complex, although ferromagnetic interactions have been observed in all other copper-azido based polymers produced with ethylene diamine reported so far.

1. Introduction

Azides are very useful for constructing magnetically coupled systems exhibiting a variety of behaviors such as antiferromagnetism [1–7], ferromagnetism [1–3,8–19], alternating ferro and antiferromagnetism [20,21], ferrimagnetism [22,23], metamagnetism [24–27], spin-canting [28], spin-flop [29], spin-glass [30], single-molecule magnetism [31–33] and single-chain magnetism [34,35]. The azido ligand is suitable bridging ligand due to its versatile binding modes and its capacity to mediate different types of magnetic exchange interactions [36–42]. In a majority of the cases, the investigations of metal-azido systems have been mainly focused on the low dimensionalities [4–7]. High-dimensional networks of metal-azido derivatives are of particular interest because of their novel topology and enhancement of bulk magnetic properties, as well as their magnetostructural correlations. In recent times the most common strategy employed for the synthesis of high-dimensional metal-azido systems is the further extension of metal-azido assemblies, using neutral organic blocking diamine co-ligands [43–47]. The simple, small diamine ligands are important in the synthesis of copper-azido cluster based polymers because they have relatively small volume. In this strategy most of the complexes were prepared by the use of blocking amine co-ligands in less than one equivalent with respect to the metal in conjunction with the azido ligand. Thus decreasing the molar amount of blocking diamine co-ligands opens more sites for the bridging azido ligand to link the metal centers and it predominantly helps by the extension of metal-azido assemblies to synthesize high-dimensional materials. Another interesting feature is that a simple change in the substitution on the diamine ligand dramatically changes the structure and magnetic behavior of the metal-azido systems [43–47]. In a systematic study Mondal and Mukherjee have synthesized three Cu(II)-azido polymers $[Cu_5(N_3)_{10}(en)_2]_n$ (**I**), $[Cu_6(N_3)_{12}(en)_4]_n$ (**II**) and $[Cu_4(N_3)_8(en)_4]_n$ (**III**) (where en = ethylenediamine) using ethylenediamine as a blocking co-ligand and they have established that the amount of the blocking amine co-ligand has a major and significant role on the structural diversity and magnetic behavior of these polymers [44]. The first two complexes are 3D polymers and the third complex is a 2D polymer. Variable-temperature magnetic studies in the temperature range 300–2 K reveal the existence of dominant ferromagnetic behavior in all three cases, with a metamagnetic type behavior in the first complex. In an another study Gu et al. have synthesized $[Cu_8(N_3)_{16}(en)_4]_n\cdot H_2O$ (**IV**) using the same diamine as blocking co-ligand [45]. This complex is also a 3D coordination polymer and shows weak ferromagnetic coupling within the copper-azido cluster units. Therefore, these systems still remain a challenging scientific endeavor.

Here, we extend the examples of polymeric copper(II) azide complexes bearing ethyenediamine as a blocking co-ligand, report-

---

* Corresponding author. Tel.: +91 33 2416 0354; fax. +91 33 2537 8797.
E-mail address: sandipsaha2000@yahoo.com (S. Saha).

0277-5387/$ - see front matter © 2010 Elsevier Ltd. All rights reserved.
doi:10.1016/j.poly.2010.09.012

ing the synthesis, X-ray crystal structure and magnetic study of a novel tetranuclear 1D polymer, $[Cu_4(N_3)_8(en)_2]_n$ (**1**).

2. Experimental

2.1. Materials and physical techniques

All reagents and solvents for the synthesis and analysis were commercially available and used as received without further purification. IR spectra were recorded as KBr pellets within the range 4000–400 cm^{-1} on a Perkin–Elmer Spectrum RXI FTIR Spectrometer. Elemental analyses were carried out using a Heraeus CHN–O-Rapid elemental analyzer. Variable-temperature magnetic susceptibility measurements were carried out on a microcrystalline sample in the 2–300 K temperature range using a Quantum Design MPMS SQUID susceptometer operating under a magnetic field of 0.1 T. Diamagnetic corrections for the complexes were estimated from Pascal's constants. The magnetic susceptibility for **1** was computed by exact calculation of the energy levels associated with the spin Hamiltonian through diagonalization of the full matrix with the enhanced version of a general program for axial symmetry [48]. Least-squares fittings were accomplished with an adapted version of the function-minimization program MINUIT [49]. The error-factor R is defined as $R = \sum \frac{(\chi_{exp}-\chi_{calc})^2}{N\chi^2_{exp}}$, where N is the number of experimental points.

2.2. Synthesis of $[Cu_4(N_3)_8(en)_2]_n$ (1)

Caution! Azido complexes of metal ions in the presence of organic ligands are potentially explosive. Only a small amount of material should be prepared, and it should be handled with care.

To a 10 mL methanolic solution of $Cu(NO_3)_2 \cdot 3H_2O$ (1.00 mmol, 241.6 mg) and en (0.50 mmol, 30 mg) an aqueous solution of NaN_3 (2.00 mmol, 130 mg) dissolved in minimum water was added slowly. The mixture was stirred for 30 min and filtered. Rectangular black crystals of **1** were obtained in two days, (yield: 70%). *Anal.* Calc. for $C_2H_8Cu_2N_{14}$: C, 6.75; H, 2.25; N, 55.16. Found: C, 7.12; H, 2.02; N, 56.1%.

2.3. X-ray crystallography

A diffraction quality single crystal of **1** was mounted on a Bruker Smart Apex II CCD Area Detector equipped with a graphite monochromator Mo Kα radiation (λ = 0.71073 Å). Data Collection was carried out using BRUKER APEX2 software [50]. Multiscan absorption correction was applied using SADABS [51]. The structure of the complex was solved by direct methods with SHELXS, and refined by full-matrix least squares based on F^2 with SHELXL [52]. All non-hydrogen atoms were refined anisotropically. The C-bound H atoms were constrained to ideal geometry and were included in the refinement in the riding model approximation. Further crystallographic analysis and figure production were carried out using PLATON99 [53] and ORTEP [54] programs. Details of the data collection parameters and crystallographic information for the complex are summarized in Table 1.

3. Results and discussion

3.1. Synthesis and IR Spectroscopy

Inspection of the $Cu^{II}/en/N_3^-$ ratios (Table 2) in the starting materials and the stoichiometry of our final product reveals excellent conformity. However, this has not always been the case for all the related complexes **I**–**IV**; except **II** where these ratios were identical. We also observe that a parameter which seems crucial in defining the nuclearity of the polymer's repeating unit is the en:N_3^- ratio; smaller such ratios (e.g., 1:10 for the octanucler **IV**) seem to favor the formation of high-nuclearity polymeric products.

Table 1
Summary of crystal data and refinement details of **1**.

Empirical formula	$C_2H_8Cu_2N_{14}$
Formula weight	355.30
Crystal dimension (mm)	0.25 × 0.22 × 0.15
Crystal system	triclinic
Space group	$P\bar{1}$
a (Å)	7.8047(14)
b (Å)	8.2059(15)
c (Å)	9.1786(16)
α (°)	86.838(3)
β (°)	84.493(4)
γ (°)	81.720(4)
V (Å^3)	578.52(18)
Z	2
T (K)	150(2)
D_{calc} (g cm^{-3})	2.040
μ (mm^{-1})	3.686
F(0 0 0)	352
θ (°)	2.23–25.00
Total data	2029
Unique data	1728
R^a	0.0511
$R_w{}^b$	0.1275
Goodness-of-fit (GOF) on F^2, S	1.028
R_{int}	0.0446
$\Delta\rho_{max}$ (e Å^{-3})	1.149
$\Delta\rho_{min}$ (e Å^{-3})	−0.808

[a] $R = \sum(|F_o - F_c|)/\sum|F_o|$.
[b] $Rw = \{R[w(|F_o - F_c|)^2]/R[w|F_o|^2]\}^{1/2}$.

However, these apply to "clean" preparations, i.e., those for which only one product is derived. Mondal and Mukherjee observed [44] that the reaction leading to **II** could also afford **III** if the initial product was left in its mother liquor. This suggests that there is a kinetic factor defining the final product, possibly relating to the relative solubilities of the different species in solution. It is conceivable that these solubilities relate to the dimensionality and nuclearity of each product.

These tentative conclusions propose possible ways of affecting the nuclearity and dimensionality of the products of this system, either through the increase of the azide ratio (for increased nuclearities), or through the solution concentration and reaction time, to control dimensionality. However, these tentative conclusions should be tested through further synthetic studies.

The IR (cm^{-1}) spectra of the complex showed absorption peaks in the range of 3300–2950 cm^{-1} which are assigned to ν_{as} (N–H) of the ethylenediamine. Peaks at 2087 and 2096 cm^{-1} are assigned to the $\nu(N_3)$ vibration of the bridging azides. Multiple peaks are indicative of multiple bridging modes of the azido ligand.

3.2. Description of the structure

The single crystal X-ray structure of complex **1** reveals doubly end-to-end azido-bridged 1D chains of Cu_4 clusters (Fig. 1). Selected bond distances and angles are listed in Table 3. The centrosymmetic Cu_4 cluster consists of two symmetry-independent Cu^{II} ions (Cu1 and Cu2) and their symmetry related counterparts. Cu1 and Cu2 are bridged end-on by the N7 and N10 nitrogen atoms of two azide ions.

Whereas Cu2 posseses an octahedral coordination environment, Cu1 possesses a distorted square-pyramidal coordination environment. Two amine nitrogens (N13 and N14) of a chelating ethylenediamine and nitrogen atoms N7 and N10 of the $\mu_{1,1}$-azides form the equatorial plane of the coordination sphere of Cu2. Atoms $N1^{ii}$ and $N6^{iii}$ of two azides occupy the axial sites of this octahe-

Table 2
Summarization of synthetic procedure for all copper-azido cluster based polymers with ethylene diamine as blocking ligand.

	$Cu(NO_3)_2{\cdot}3H_2O$ (mg/mmol)	Ethylene diamine (mg/mmol)	NaN_3 (mg/mmol)	Cu/en/N_3^- (starting materials)	Cu/en/N_3^- (product)	Solvent (s)	*T* (°C)	Required time (h; days)	Compounds	Dimensionality	Refs.
I	302/1.25	15.0/0.25	162/2.50	5:1:10	5:2:10	MeOH/H_2O	Stirred 15 min at 60 °C	12 h	$[Cu_5(N_3)_{10}(en)_2]_n$	3	[44]
II	241.6/1.0	40/0.66	130/2.0	3:2:6	3:2:6	MeOH/H_2O	RT	2 days	$[Cu_6(N_3)_{12}(en)_4]_n$	3	[44]
III	idem	idem	idem	idem	1:1:2	MeOH/H_2O	RT	6 days	$[Cu_4(N_3)_8(en)_4]_n$	2	
III	483.2/2.0	130/2.0	130/2.0	1:1:1	1:1:2	MeOH/H_2O	RT	10 days	$[Cu_4(N_3)_8(en)_4]_n$	2	[44]
IV	241.6/1.0	60/1.0	650/10.0	1:1:10	2:1:4	MeOH	Kept at 5 °C	15 days	$[Cu_8(N_3)_{16}(en)_4]_n{\cdot}H_2O$	3	[45]
1	241.6/1.0	30/0.5	130/2.0	2:1:4	2:1:4	MeOH/H_2O	RT	2 days	$[Cu_4(N_3)_8(en)_2]_n$	1	Our study

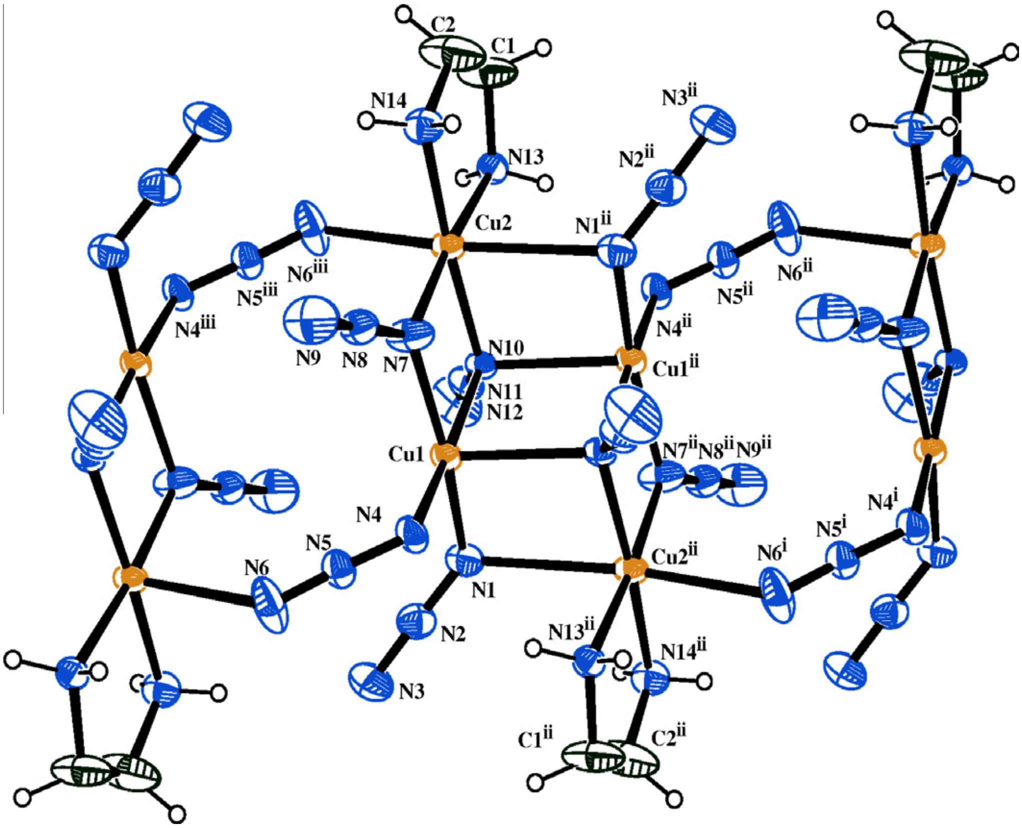

Fig. 1. The ORTEP diagram (30% ellipsoidal probability) of the azido bridged polymeric chains of Cu4 clusters in **1** (i = 1 + *x*, *y*, *z*; ii = 2 − *x*, −*y*, 1 − *z*; iii = 1−*x*, −*y*, 1 − *z*).

dron. Atoms N1, N7 and N10 and of three end-on azides, along with N4 of an end-to-end azide ions form the basal plane of the square pyramidal coordination environment of Cu1. $N10^{ii}$ occupies the apex of this square pyramid.

Cu1 and Cu2 form a pair, sharing a common edge, and these pairs form the centrosymmetric Cu_4 cluster through end-on azide bridges, linking apical-equatorial and basal-axial positions of the octahedral-square pyramidal pairs. This combination of coordination of the bridges affects significantly the magnetic couplings within the cluster. The Cu_4 units are finally bridged by two end-to-end azides, each connecting a basal coordination position of Cu1 with an axial position of the symmetry counterpart of Cu2. The axial bond lengths of Cu1–N10_b, Cu2–N6_a and Cu2–N1_b are 2.437(4), 2.465(6) and 2.744(5) Å, respectively, which are significantly longer than those for their corresponding equatorial Cu–N bonds [Cu1–N1, Cu1–N4, Cu1–N7, Cu1–N10 ranging from 1.972(5) to 2.030(4) Å and Cu2–N7, Cu2–N10, Cu2–N13, Cu2–N14 ranging from 1.987(5) to 2.018(4) Å], indicating the presence of a strong Jahn-Teller effect [47]. The Cu–N_{en} distances [Cu2–N13 2.002(4) Å and Cu2–N14 1.997(5) Å] are consistent with those for other ethylene diamine-copper complexes [44]. The Cu–N_{az}–Cu bond angles between Cu1 and Cu2 [Cu1–N7–Cu2 and Cu1–N10–Cu2] are 102.1(3) and 99.70(17)°, respectively.

Azido bridged polymeric chains of Cu_4 units run along crystallographic *a*-axis and are aligned parallely in the *ac*-plane (Fig. 2). This parallel alignment is facilitated by hydrogen bonding between the $-NH_2$ donor and azide acceptors (Fig. 3 and Table 4). As shown in Fig. 3, a cyclic hydrogen bonding pattern ($R_2^2(8)$ in Etter's graph

Table 3
Selected bond distances (Å) and angles (°) for complex **1**.

Cu1–N1	1.972(5)	N5–N6	1.149(7)
Cu1–N4	1.973(4)	N7–N8	1.199(7)
Cu1–N7	1.992(6)	N8–N9	1.116(9)
Cu1–N10	2.030(4)	N10–N11	1.266(6)
Cu1–N10_b	2.437(4)	N11–N12	1.117(9)
Cu2–N7	1.987(5)		
Cu2–N10	2.018(4)		
Cu2–N13	2.002(4)		
Cu2–N14	1.997(5)		
Cu2–N6_a	2.465(6)		
Cu2–N1_b	2.744(5)		
N1–N2	1.192(7)		
N2–N3	1.156(8)		
N4–N5	1.201(6)		
N1–Cu1–N4	95.57(19)	N1–N2–N3	177.6(6)
N1–Cu1–N7	166.2(2)	Cu1–N4–N5	120.5(3)
N1–Cu1–N10	92.55(18)	N4–N5–N6	176.1(5)
N1–Cu1–N10_b	90.92(16)	Cu2_a–N6–N5	133.2(4)
N4–Cu1–N7	93.5(2)	Cu1–N7–Cu2	102.1(3)
N4–Cu1–N10	171.63(17)	Cu1–N7–N8	124.4(4)
N4–Cu1–N10_b	94.88(15)	Cu2–N7–N8	131.6(4)
N7–Cu1–N10	78.89(18)	N7–N8–N9	178.8(7)
N7–Cu1–N10_b	98.6(2)	Cu1–N10–Cu2	99.70(17)
N10–Cu1–N10_b	82.93(15)	Cu1–N10–N11	119.7(3)
N7–Cu2–N10	79.3(2)	Cu1–N10–Cu1_b	97.07(16)
N7–Cu2–N13	174.9(2)	Cu2–N10–N11	123.8(3)
N7–Cu2–N14	97.8(2)	Cu1_b–N10–Cu2	97.42(15)
N6_a–Cu2–N7	97.4(2)	Cu1_b–N10–N11	114.0(3)
N1_b–Cu2–N7	92.3(2)	N10–N11–N12	175.9(6)
N10–Cu2–N13	96.57(17)	Cu2–N13–C1	109.1(4)
N10–Cu2–N14	173.49(18)	Cu2–N14–C2	107.7(4)
N6_a–Cu2–N10	98.25(19)	Cu2–N13–H13B	110.00
N1_b–Cu2–N10	81.57(15)	C1–N13–H13A	110.00
N13–Cu2–N14	85.99(19)	Cu2–N13–H13A	110.00
N6_a–Cu2–N13	86.02(18)	H13A–N13–H13B	108.00
N1_b–Cu2–N13	84.20(15)	C1–N13–H13B	110.00
N6_a–Cu2–N14	87.9(2)	Cu2–N14–H14B	110.00
N1_b–Cu2–N14	92.76(17)	Cu2–N14–H14A	110.00
N1_b–Cu2–N6_a	170.13(17)		
Cu1–N1–N2	121.1(4)		
Cu1–N1–Cu2_b	89.26(17)		
Cu2_b–N1–N2	126.3(4)		

a = 1−*x*, −*y*, 1 − *z*; *b* = 2 − *x*, −*y*, 1 − *z*.

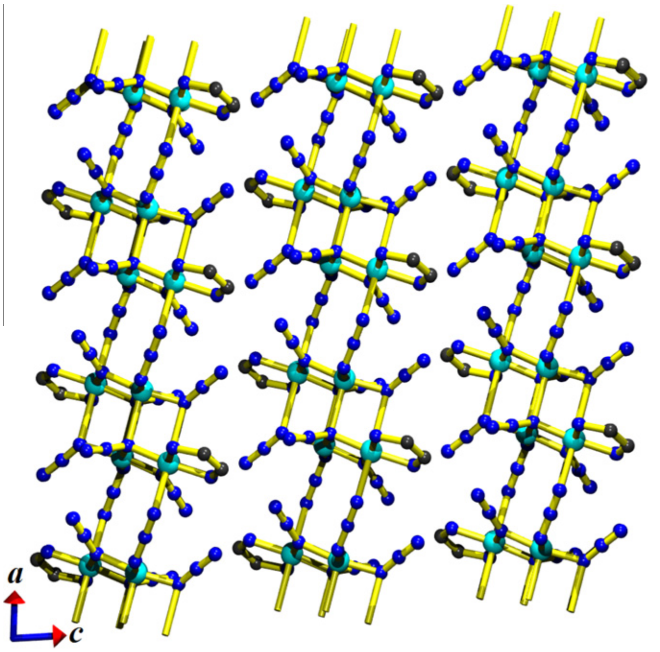

Fig. 2. Packing arrangement of polymeric chains in **1**.

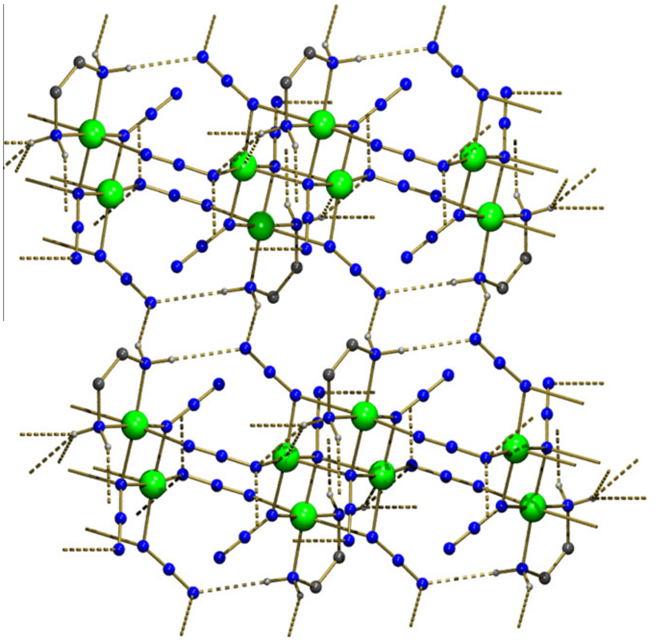

Fig. 3. Hydrogen bonding between amine and azide groups in **1**.

notation) between these groups joins parallel polymeric chains along crystallographic *c*-axis. One of the amino groups (N14 nitrogen) of the chelating ethylene diamine ligand takes part in this centrosymmetric cyclic hydrogen bonding pattern where both of its protons are attached to N3 terminal nitrogen atoms of end-on bridging azides from adjacent polymeric chains. The other amino group (N13 nitrogen) also forms strong bifurcated hydrogen bonds donating H13A protons simultaneously to N4 of end-to-end bridging azide and N12 of end-on bridging azide, respectively. The other proton (H13B) is also donated to the same N4 nitrogen but with a different symmetry location (*x*, 1 + *y*, *z*) on a different polymeric chain. This establishes supramolecular connection between adjacent polymeric chains of Cu_4 clusters along the crystallographic *b*-axis. Thus the overall packing is the result of a hydrogen-bonded supramolecular assembly of 1D polymeric chains of Cu_4 clusters whose compact arrangement is facilitated by $-NH_2$ group assisted hydrogen bonding among these chains in other two crystallographic directions. This hydrogen bonding pattern is responsible for the respective optimal alignment of the azide ions which, in turn, fixes the geometrical angle parameters of the magnetic exchange pathway.

3.3. Magnetic properties

$\chi_M T$ versus *T* data for **1** are shown in Fig. 4. The $\chi_M T$ product of **1** at 300 K is 1.82 $cm^3\ mol^{-1}$ K, close to the value expected for four non-interacting $S = 1/2$ ions ($g = 2.2$). This shows a slow decrease upon cooling down to 100 K, below which temperature the decrease accelerates, reaching a value of 0.33 $cm^3\ mol^{-1}$ K at 2 K. This behaviour suggests the interplay of weak antiferromagnetic interactions. *M* versus *H* measurements at 2 K show no signs of saturation up to 5.5 T, indicating the presence of exchange coupling over an extended magnetic system.

Based on the crystal structure of **1**, we may view the complex as a series of centrosymmetric defective double cubanes (Fig. 5). From this analysis, a rigorous interpretation of the magnetic behaviour of **1** would require the consideration of four exchange pathways, namely $J_1 = J_{\mathrm{Cu1Cu2}} = J_{\mathrm{Cu1'Cu2'}}$, $J_2 = J_{\mathrm{Cu1Cu2'}} = J_{\mathrm{Cu1'Cu2}}$, $J_3 = J_{\mathrm{Cu1Cu1'}}$ and $J_4 = J_{\mathrm{Cu1Cu2''}} = J_{\mathrm{Cu1''Cu2}}$ (Fig. 5). Since a polymeric structure with such

Table 4
Hydrogen bond parameters (Å, °).

D–H···A	D–H (Å)	H···A (Å)	D···A (Å)	<D–H···A (°)	Symmetry
N13–H13A···N4	0.90	2.47	3.291(6)	153	2 − *x*, −*y*, 1 − *z*
N13–H13A···N12	0.90	2.58	3.135(9)	121	2 − *x*, 1 − *y*, 1 − *z*
N13–H13B···N4	0.90	2.39	3.252(6)	161	*x*, 1 + *y*, *z*
N14–H14A···N3	0.90	2.50	3.391(8)	170	1 − *x*, −*y*, 1 − *z*
N14–H14B···N3	0.90	2.50	3.333(8)	154	*x*, *y*, 1 + *z*
C2–H2B···N12	0.97	2.44	3.340(12)	155	*x*, *y*, 1 + *z*

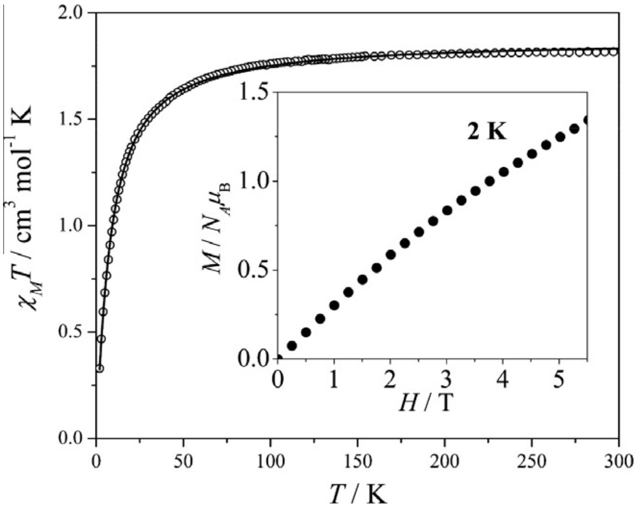

Fig. 4. $\chi_M T$ vs *T* data for **1**, along with the calculated curve from solution **F** (see text). Isothermal magnetization data at 2 K are shown in the inset.

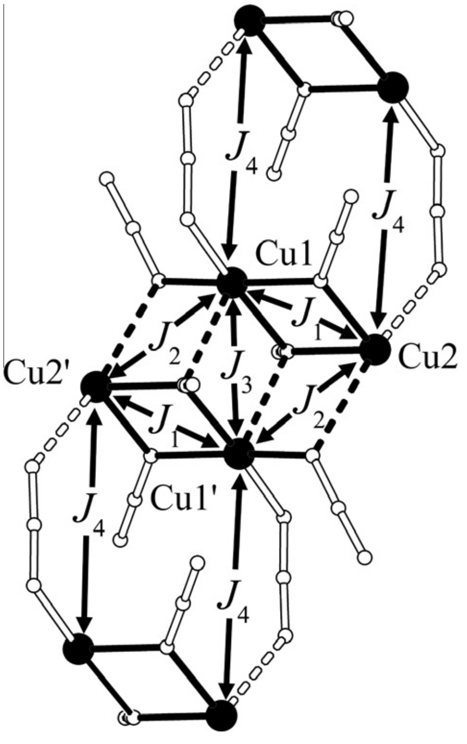

Fig. 5. Spin-coupling scheme for **1**.

a complicated exchange coupling scheme is not amenable to analytical treatment, simplifications are required to make its analysis tractable. The most obvious such simplification is to treat the inter-tetranuclear exchange interactions, J_4, as perturbations using a mean-field correction, thus considering **1** as an array of weakly interacting tetranuclear clusters. Although this simplification, depending on the strength of J_4, may not be entirely valid, it is indispensible if any quantitative interpretation is to be attempted. Moreover, it is found that this bridging is accomplished by end-on azides coordinated to a basal coordination position of Cu1 and to an axial coordination position of Cu2. Thus, any eventual magnetic exchange will have to be transmitted through a superexchange pathway comprising one magnetic orbital (on Cu1) and one non-magnetic orbital (on Cu2). It is therefore plausible to assume that it will be relatively weak.

Therefore, the Hamiltonian considered was:

$$\hat{H} = -2[J_1(\hat{\mathbf{S}}_{\mathrm{Cu1}}\hat{\mathbf{S}}_{\mathrm{Cu2}} + \hat{\mathbf{S}}_{\mathrm{Cu1'}}\hat{\mathbf{S}}_{\mathrm{Cu2'}}) + J_2(\hat{\mathbf{S}}_{\mathrm{Cu1}}\hat{\mathbf{S}}_{\mathrm{Cu2'}} + \hat{\mathbf{S}}_{\mathrm{Cu1'}}\hat{\mathbf{S}}_{\mathrm{Cu2}}) \\ + J_3\hat{\mathbf{S}}_{\mathrm{Cu1}}\hat{\mathbf{S}}_{\mathrm{Cu1'}}] - 2zjS_z\langle S_z\rangle$$

As described above, pairs Cu1–Cu1$^{\mathrm{ii}}$, Cu1–Cu2$^{\mathrm{ii}}$ and Cu2–Cu1$^{\mathrm{ii}}$ are all bridged by azides coordinated to one position occupying a magnetic orbital (basal or equatorial) and to one position occupying a non-magnetic orbital (axial or apical). Only the Cu1–Cu2 pair is bridged by azides coordinated to positions occupying magnetic orbitals on both ions (basal). Given the fact that only interaction J_1 is propagated through a superexchange pathway involving magnetic orbitals of both Cu ions, it has the potential to be the strongest of all, depending of course on various structural parameters, like the Cu–N$_{\mathrm{azide}}$–Cu angle, that may modulate its magnitude (see Section 3). In any case, however, all other interactions are expected to be quite weak, if indeed operative. Due to the complexity of the system, and in order to facilitate its treatment, we decided to use the assumption of J_1 being the strongest interaction as our starting point. Nevertheless, other solutions were also considered.

In order to establish whether all other interactions are of significant strength, initial fitting attempts were carried out by fixing them to zero. These attempts did not yield satisfactory fits, so it was concluded that other interactions are also operative. However, in order to avoid overparametrizing our problem, we avoided liberating all variables simultaneously.

When *zj* was fixed to zero, fits yielded two solutions of acceptable quality: $J_1 = -3.7$ cm^{-1}, $J_2 \sim 0$, $J_3 = -7.1$ cm^{-1}, $g = 2.22$, with $R = 1.9 \times 10^{-4}$ (solution **A**) and $J_1 \sim J_2 = -3.2$ cm^{-1}, $J_3 = -4.9$ cm^{-1}, $g = 2.23$, with $R = 2.0 \times 10^{-4}$ (solution **B**).

When *zj* was released, we conducted fits with J_2 or J_3 (or both) fixed to zero. These attempts yielded best-fit solutions: $J_1 = -0.24$ cm^{-1}, $J_2 = -1.1$ cm^{-1}, $J_3 = 0$ (fixed), $zj = -1.9$ cm^{-1}, $g = 2.25$, with $R = 1.0 \times 10^{-4}$ (solution **C**), $J_1 = -1.2$ cm^{-1}, $J_2 = 0$ (fixed), $J_3 \sim 0$, $zj = -1.9$ cm^{-1}, $g = 2.25$, with $R = 1.0 \times 10^{-4}$ (solution **D**), $J_1 = -1.1$ cm^{-1}, $J_2 = J_3 = 0$ (fixed), $zj = -1.9$ cm^{-1}, $g = 2.25$, with $R = 1.0 \times 10^{-4}$ (solution **E**), $J_1 = +4.2$ cm^{-1}, $J_2 \sim 0$, $J_3 = 0$ (fixed), $zj = -2.6$ cm^{-1}, $g = 2.23$, with $R = 3.2 \times 10^{-4}$ (solution **F**) and $J_1 = +0.33$ cm^{-1}, $J_2 = 0$ (fixed), $J_3 = +9.4$ cm^{-1}, $zj = -2.6$ cm^{-1}, $g = 2.23$, with $R = 1.8 \times 10^{-5}$ (solution **G**).

Given our above reasoning on the magnitudes of J_1, J_2 and J_3, we discard solutions **A** and **B**, since they involve relatively high J_3 values. This means that we are required to take *zj* into account.

On the same grounds, solution **G** must also be discarded, since it yields too high a J_3 value. All remaining solutions (**C**, **D**, **E** and **F**) entail practically zero values for both J_2 and J_3, with **C**, **D** and **E** corresponding to $J_1 < 0$ and **F** to $J_1 > 0$.

Kahn had calculated that accidental orthogonality for Cu–N_{azide}–Cu bridges occurs at a crossover angle of 103° [55], and subsequently Ruiz et al. calculated this angle to be 104° [41]. The respective Cu1–N7–Cu2 and Cu1–N10–Cu2 angles in **1**, are 102.1 and 99.7°, respectively, i.e., significantly below these crossover angles. This would tend to support solution **F**, i.e., a moderately ferromagnetic interaction. In the case of a ferromagnetic J_1, the overall antiferromagnetic behavior could then be assigned to the collective effect of the weak, but numerous, intercluster antiferromagnetic interactions. However, this is suggested as a tentative conclusion due to the complexity of our spin system; the physical meaning of the presented solutions strongly hinges upon the validity of our initial assumption, i.e., considering that the intercluster interactions (J_4) are weak enough to be treated as perturbations using a mean-field approximation. Consideration of the dihedral angle formed by the basal planes of Cu1 and $Cu1^{ii}$ also favors the above conclusion: due to symmetry, this angle is zero.

A final point worth noting is that the overall antiferromagnetic behavior of **1** is at variance with the observed behavior of the previously reported complexes **I**–**IV**, all of which exhibit overall ferromagnetism. Complete magnetostructural comparisons are beyond the scope of the present work, but we might note that the presence of end-on bridges with small Cu–N–Cu angles may be a favorable factor for the observation of ferromagnetism in copper-azide systems. At a first level of approximation this may be corroborated by the presence of very acute Cu–N–Cu angles in **I** (∼83.2°) and **IV** (∼88.5°), the complexes exhibiting the most distinctively ferromagnetic behavior. Such structural elements are absent in the antiferromagnetic **1**, which exhibits more obtuse respective angles, particularly those affecting J_1.

4. Conclusion

In summary, a new 1D copper(II)-azide polymer based on the tetranuclear copper cluster $[Cu_4(N_3)_8(en)_2]_n$ (**1**) has been synthesized and characterized by elemental analyses, IR spectroscopy, X-ray crystallography and variable-temperature magnetic susceptibility studies. X-ray crystal structure determination reveals that the structure consists of chains of a centrosymmetric tetranuclear copper(II)-azido cluster. In turn, these tetranuclear clusters are connected with each other through double azido end-to-end bridges to form the one dimensional chain. Variable-temperature magnetic studies indicate an antiferromagnetic overall behavior. Due to the complexity of the spin system the precise factors cannot be derived with certainty, but we may propose that the intercluster antiferromagnetic interactions, even if weak, may be instrumental in defining this overall behavior, even if interaction J_1 is ferromagnetic.

5. Supplementary data

CCDC 787342 contains the supplementary crystallographic data for **1**. These data can be obtained free of charge via http://www.ccdc.cam.ac.uk/conts/retrieving.html, or from the Cambridge Crystallographic Data Centre, 12 Union Road, Cambridge CB2 1EZ, UK; fax: (+44) 1223-336-033; or email: deposit@ccdc.cam.ac.uk.

Acknowledgements

Financial support from UGC [Sanction No. F.38-5/2009(SR)] and DST [Sanction No. SR/FT/CS-060/2009], New Delhi to S.S. are gratefully acknowledged.

References

[1] J. Ribas, A. Escuer, M. Monfort, R. Vicente, R. Cortes, L. Lezama, T. Rojo, Coord. Chem. Rev. 193–195 (1999) 1027. and references cited therein.
[2] A. Escuer, G. Aromí, Eur. J. Inorg. Chem. (2006) 4721. and references cited therein.
[3] Y.-F. Zeng, X. Hu, C.-F. Liu, X.-H. Bu, Chem. Soc. Rev. 38 (2009) 469. and references cited therein.
[4] S. Koner, S. Saha, K.-I. Okamato, J.-P. Tuchagues, Inorg. Chem. 42 (2003) 4668.
[5] S. Koner, S. Saha, T. Mallah, K.-I. Okamato, Inorg. Chem. 43 (2004) 840.
[6] S. Saha, S. Koner, J.-P. Tuchagues, A.K. Boudalis, K.-I. Okamato, S. Banerjee, D. Mal, Inorg. Chem. 44 (2005) 6379.
[7] M. Zibri, S. Saha, C. Adhikary, S. Chaudhuri, C. Daul, S. Koner, Inorg. Chim. Acta 359 (2006) 1193.
[8] A. Escuer, R. Vicente, F.A. Mautner, M.A.S. Goher, M. A.M. Abu-Youssef, Chem. Commun. (2002) 64.
[9] T.C. Stamatatos, K.A. Abboud, W. Wernsdorfer, G. Christou, Angew. Chem., Int. Ed. 45 (2006) 4134.
[10] A.M. Ako, I.J. Hewitt, V. Mereacre, R. Clérac, W. Wernsdorfer, C.E. Anson, A.K. Powell, Angew. Chem., Int. Ed. 45 (2006) 4926.
[11] A. Escuer, M.A.S. Goher, F.A. Mautner, R. Vicente, Inorg. Chem. 39 (2000) 2107.
[12] Z. Shen, J.-L. Zuo, S. Gao, Y. Song, C.-M. Che, H.-K. Fun, X.-Z. You, Angew. Chem., Int. Ed. 39 (2000) 3633.
[13] S. Martin, M.G. Barandika, L. Lezama, J.L. Pizarro, Z.E. Serna, J.I. Ruiz de Larramendi, M.I. Arriortua, T. Rojo, R. Cortés, Inorg. Chem. 40 (2001) 4109.
[14] A. Escuer, J. Cano, M.A.S. Goher, Y. Journaux, F. Lloret, F.A. Mautner, R. Vicente, Inorg. Chem. 39 (2000) 4688.
[15] Y.-F. Zeng, F.-C. Liu, J.-P. Zhao, S. Cai, X.-H. Bu, J. Ribas, Chem. Commun. (2006) 2227.
[16] J.L. Manson, A.M. Arif, J.S. Miller, Chem. Commun. (1999) 1479.
[17] C.S. Hong, J.-E. Koo, S.-K. Son, Y.S. Lee, Y.-S. Kim, Y. Do, Chem. Eur. J. 7 (2001) 4243.
[18] F.-C. Liu, Y.-F. Zeng, J.-R. Li, X.-H. Bu, H.-J. Zhang, J. Ribas, Inorg. Chem. 44 (2005) 7298.
[19] F.-C. Liu, Y.-F. Zeng, J.-P. Zhao, B.-W. Hu, E.C. Sañudo, J. Ribas, X.-H. Bu, Inorg. Chem. 46 (2007) 7698.
[20] C.-M. Liu, S. Gao, D.-Q. Zhang, Y.-H. Huang, R.-G. Xiong, Z.-L. Liu, F.-C. Jiang, D.-B. Zhu, Angew. Chem., Int. Ed. 43 (2004) 990.
[21] M.A.S. Goher, J. Cano, Y. Journaux, M.A.M. Abu-Youssef, F.A. Mautner, A. Escuer, R. Vicente, Chem. Eur. J. 6 (2000) 778.
[22] M.A.M. Abu-Youssef, A. Escuer, M.A.S. Goher, F.A. Mautner, G.J. Reib, R. Vicente, Angew. Chem., Int. Ed. 39 (2000) 1624.
[23] A. Escuer, R. Vicente, M.S. El Fallah, M.A.S. Goher, F.A. Mautner, Inorg. Chem. 37 (1998) 4466.
[24] A. Das, G.M. Rosair, M.S. El Fallah, J. Ribas, S. Mitra, Inorg. Chem. 45 (2006) 3301.
[25] Z. He, Z.-M. Wang, S. Gao, C.-H. Yan, Inorg. Chem. 45 (2006) 6694.
[26] M. Monfort, I. Resino, J. Ribas, H. Stoeckli-Evans, Angew. Chem., Int. Ed. 39 (2000) 191.
[27] G. Lazari, T.C. Stamatatos, C.P. Raptopoulou, V. Psycharis, M. Pissas, S.P. Perlepes, A.K. Boudalis, Dalton Trans. (2009) 3215.
[28] H.H. Ko, J.H. Lim, H.C. Kim, C.S. Hong, Inorg. Chem. 45 (2006) 8847.
[29] Y.S. You, J.H. Yoon, H.C. Kim, C.S. Hong, Chem. Commun. (2005) 4116.
[30] X.-T. Liu, X.-Y. Wang, W.-X. Zhang, P. Cui, S. Gao, Adv. Mater. 18 (2006) 2852.
[31] A.K. Boudalis, Y. Sanakis, J.M. Clemente-Juan, B. Donnadieu, V. Nastopoulos, A. Mari, Y. Coppel, J.-P. Tuchagues, S.P. Perlepes, Chem. Eur. J. 14 (2008) 2514.
[32] T.C. Stamatatos, K.A. Abboud, W. Wernsdorfer, G. Christou, Angew. Chem., Int. Ed. 46 (2007) 884.
[33] C.-I. Yang, W. Wernsdorfer, G.-H. Lee, H.-L. Tsai, J. Am. Chem. Soc. 129 (2007) 456.
[34] X.-Y. Wang, Z.-M. Wang, S. Gao, Chem. Commun. (2008) 281.
[35] T.-F. Liu, D. Fu, S. Gao, Y.-Z. Zhang, H.L. Sun, G. Su, Y.-J. Liu, J. Am. Chem. Soc. 125 (2003) 13976.
[36] E.-Q. Gao, S.-Q. Bai, Z.-M. Wang, C.-H. Yan, J. Am. Chem. Soc. 125 (2003) 4984.
[37] E.-Q. Gao, Y.-F. Yue, S.-Q. Bai, Z. He, C.-H. Yan, J. Am. Chem. Soc. 126 (2004) 1419.
[38] Z.-G. Gu, Y. Song, J.-L. Zuo, X.-Z. You, Inorg. Chem. 46 (2007) 9522.
[39] L.K. Thompson, S.S. Tandon, F. Lloret, J. Cano, M. Julve, Inorg. Chem. 36 (1997) 3301.
[40] S.S. Tandon, L.K. Thompson, M.E. Manuel, J.N. Bridson, Inorg. Chem. 33 (1994) 5555.
[41] E. Ruiz, J. Cano, S. Alvarez, P. Alemany, J. Am. Chem. Soc. 120 (1998) 11122.
[42] F. Fabrizi de Biani, E. Ruiz, J. Cano, J.J. Novoa, S. Alvarez, Inorg. Chem. 39 (2000) 3221.
[43] Z.-G. Gu, J. -L. Zuo, X.-Z. You, Dalton Trans. (2007) 4067.
[44] K.C. Mondal, P.S. Mukherjee, Inorg. Chem. 47 (2008) 4215.
[45] Z.-G. Gu, Y.-F. Xu, X.-J. Yin, X.-H. Zhou, J.-L. Zuo, X.-Z. You, Dalton Trans. (2008) 5593.
[46] S. Mukherjee, B. Gole, R. Chakrabarty, P.S. Mukherjee, Inorg. Chem. 48 (2009) 11325.
[47] C.-B. Tian, Z.-H. Li, J.-D. Lin, S.-T. Wu, S.-W. Du, P. Lin, Eur. J. Inorg. Chem. (2010) 427.
[48] J.-M. Clemente-Juan, C. Mackiewicz, M. Verelst, F. Dahan, A. Bousseksou, Y. Sanakis, J.-P. Tuchagues, Inorg. Chem. 41 (2002) 1478.
[49] F. James, M. Roos, Comput. Phys. Commun. 10 (1975) 343.

[50] APEX2, version 2.2. Bruker AXS Inc., Madison, WI, 2006.

[51] G.M. Sheldrick, SADABS, Programs for Area Detector Adsorption Correction, Institute for Inorganic Chemistry, University of Göttingen, Germany, 1996.

[52] G.M. Sheldrick, SHELXTL, version 5.1, Program for the Solution and Refinement of Crystal Structures, Bruker AXS Inc., Madison, WI, 1999.

[53] A.L. Spek, PLATON, Molecular Geometry Program, University of Utrecht, The Netherlands, 1999.

[54] L.J. Farrugia, J. Appl. Crystallogr. 30 (1997) 565.

[55] O. Kahn, Inorg. Chim. Acta 62 (1982) 3.